



Published in final edited form as:

Acad Radiol. 2012 August ; 19(8): . doi:10.1016/j.acra.2012.03.017.

Systems for Lung Volume Standardization during Static and Dynamic MDCT-based Quantitative Assessment of Pulmonary Structure and Function

Matthew K. Fuld, B.S.^{1,2}, Randall Grout, B.S.¹, Junfeng Guo, Ph.D.^{1,2}, John H. Morgan, B.S.¹, and Eric A. Hoffman, Ph.D.^{1,2}

¹Department of Radiology, University of Iowa

²Department of Biomedical Engineering, University of Iowa

Abstract

Rationale and Objectives—Multidetector-row Computed Tomography (MDCT) has emerged as a tool for quantitative assessment of parenchymal destruction, air trapping (density metrics) and airway remodeling (metrics relating airway wall and lumen geometry) in chronic obstructive pulmonary disease (COPD) and asthma. Critical to the accuracy and interpretability of these MDCT-derived metrics is the assurance that the lungs are scanned during a breath-hold at a standardized volume.

Materials and Methods—A computer monitored turbine-based flow meter system was developed to control patient breath-holds and facilitate static imaging at fixed percentages of the vital capacity. Due to calibration challenges with gas density changes during multi-breath xenon-CT an alternative system was required. The design incorporated dual rolling seal pistons. Both systems were tested in a laboratory environment and human subject trials.

Results—The turbine-based system successfully controlled lung volumes in 32/37 subjects, having a linear relationship for CT measured air volume between repeated scans: for all scans, the mean and confidence interval of the differences (scan1-scan2) was -9 ml ($-169, 151$); for TLC alone 6 ml ($-164, 177$); for FRC alone, -23 ml ($-172, 126$). The dual-piston system successfully controlled lung volume in 31/41 subjects. Study failures related largely to subject non-compliance with verbal instruction and gas leaks around the mouthpiece.

Conclusion—We demonstrate the successful use of a turbine-based system for static lung volume control and demonstrate its inadequacies for dynamic xenon-CT studies. Implementation of a dual-rolling seal spirometer has been shown to adequately control lung volume for multi-breath wash-in xenon-CT studies. These systems coupled with proper patient coaching provide the tools for the use of CT to quantitate regional lung structure and function. The wash-in xenon-CT method for assessing regional lung function, while not necessarily practical for routine clinical

© 2012 The Association of University Radiologists. Published by Elsevier Inc. All rights reserved.

Contact Information: Eric A. Hoffman, Division of Physiological Imaging, University of Iowa Hospitals & Clinics, 200 Hawkins Drive, CC 701 GH, Iowa City, IA 52241, eric-hoffman@uiowa.edu.

Disclosure

Eric Hoffman is a founder and shareholder in VIDA diagnostics, which is commercializing lung image analysis software derived by the University of Iowa lung-imaging group. Junfeng Guo is also a shareholder in VIDA diagnostics.

Publisher's Disclaimer: This is a PDF file of an unedited manuscript that has been accepted for publication. As a service to our customers we are providing this early version of the manuscript. The manuscript will undergo copyediting, typesetting, and review of the resulting proof before it is published in its final citable form. Please note that during the production process errors may be discovered which could affect the content, and all legal disclaimers that apply to the journal pertain.

studies, provides for a dynamic protocol against which newly emerging single breath, dual-energy xenon-CT measures can be validated.

Keywords

Lung volume control; xenon-CT; dual-energy CT

Introduction

Multidetector-row Computed Tomography (MDCT) has emerged as a tool for quantitation of parenchymal destruction, air trapping and airway remodeling in chronic obstructive pulmonary disease (COPD) and asthma (1–8). Critical to the accuracy and interpretability of these metrics is the assurance that the lungs are scanned during a breath-hold at a standardized volume (9). Methods have been reported in which correction factors are proposed for inconsistent lung volumes (10,11). However, there is no replacement for accurate control of lung volume at the time of scanning.

In addition to structural-based measurements, wash-in xenon-CT enables the measurement of regional ventilation by utilizing the increase in measured density of a region of interest caused by the wash-in of radiodense xenon gas. This method has proved reliable in animal studies (12–15), and because the animals were anesthetized the anesthetic properties of xenon were not a problem (16,17). Animals were mechanically ventilated thus it was very straightforward to scan at a repeatable set of respiratory pauses as xenon gas was washed into and out of the lungs. The goal for measuring ventilation in humans is to capture the dynamic nature of ventilation in awake, free-breathing subjects. This therefore necessitates the use of a lower concentration of xenon gas and identifying repeatable pause points in sequential respiratory cycles when axial scans can be acquired. Currently a 30% xenon / 70% oxygen mixture is used for safety purposes, though a mixture which also includes krypton would be preferred (18). However, the introduction of gases of varying densities complicates the tracking of gas flow at the mouth with standard respiratory gas flow meters. With the emergence of dual-energy computed tomography methods for single breath xenon-based assessment of regional lung function have been reported (19,20). However, there have been no reports validating these single breath techniques against a method that assesses true regional ventilation. The dynamic volume control approach we present here provides for such a comparator.

To yield an accurate measure of regional ventilation the dynamic wash-in xenon-CT method requires subjects to precisely achieve the same end-expiratory lung volume repeatedly over multiple breaths. When asked to maintain a consistent end-expiratory lung volume most subjects have modest difficulty even when they are being monitored and coached. Additionally, the slight anesthetic effect of xenon, even at 30%, represents an extra hurdle to overcome.

Many methods for lung volume control have been tried including belt systems and pressure drop pneumotachometers (21–25), each with varying degrees of success. When monitoring changes in the rib cage to estimate changes in lung volume, it has been shown that one must take into account shifts between rib cage and diaphragm breathing (26,27).

Devices for measuring in-line air movement suitable for use in conjunction with CT scanning include pressure-drop pneumotachometers, hot-wire anemometers, ultrasonic transducers, and turbine-based flow meters (28). Pressure-drop pneumotachometers are widely used, however they suffer from a number of drawbacks stemming from difficulties in calibration. A volumetric flow rate signal is generated from the pressure drop across the permeable screen; this signal is then integrated to determine volume. Minor errors in zeroing

may cause volume creep over time. The devices are linear under a specific set of calibrated conditions; changes in humidity, temperature, or gas composition will cause invalid measurements. Since the eventual goal is to create a system suitable for lung volume control during both static breath-hold imaging and dynamic wash-in multi-breath xenon-CT scans, it was decided that an alternative to a pressure-drop pneumotachometer was required.

We present here solutions for lung volume control to facilitate: 1) static breath-holds and 2) intermittent breath-holds within a multi-breath imaging sequence in which gas density varies on expiration.

Materials and Methods

In order to achieve both types of lung volume control two systems were developed and tested.

Breath-hold Lung Volume Control

Turbine-Based Breath-hold System Design—The lung volume control system, comprised of a mouthpiece, filter, turbine-based airflow measurement device, balloon occlusion valve and integrated software control, is calibrated via a slow vital capacity (SVC) maneuver with a display visible to the system operator for coaching and control purposes (Figure 1-A). The primary component in the system is the VMM-400, a turbine-based flow meter (Interface USA, Laguna Niguel, CA) (Figure 1-B). The turbine relies on the rotation of an extremely low friction impeller spinning due to air movement. One rotation of the impeller indicates a specific volume passing through the circuit. This volume depends on the size of the chosen insert used; in this case the small turbine was used to obtain the highest volume resolution (0.5 mL increments). To assist subjects during breath-hold procedures, an inflatable balloon-type 2-way shutoff valve (9430 series, Hans Rudolph, Shawnee, KS) is placed between the turbine and the system's end; the valve is controlled remotely (Figure 1-C). It can be set to automatically inflate as the subject approaches a particular lung volume or can be manually inflated by the operator in the control room with a click of a button. The balloon is inflated with helium rather than compressed room air to achieve the minimum response time. As this is a pressure-inflated balloon valve, it is meant as an assist to timing and comfort of the patient, but in the case of an emergency the balloon can be overwhelmed by a forceful effort from the patient. Reusable, sterilizable mouthpieces are connected to single use bacterial viral filters, placed between the patient and the turbine. To comfortably position the breathing circuit during the scan, a clamp holds the circuit above the patient using an articulating locking arm (CIVCO, Kalona, IA).

To combine the components into an easy to use device, a custom computer control system was developed in the LabVIEW 8.0 platform (National Instruments, Austin, TX) (Figure 2). The system utilizes a data acquisition board to capture the digital counter signal from the turbine and an on/off signal signifying x-ray on while also outputting a signal to trigger the solenoid valve controlling balloon inflation. The procedure for acquiring a volume controlled scan involves a series of system calibrations and breathing maneuvers directed by the system operator (Figure 3).

Turbine-Based Breath-hold System Calibration and Testing—Initially, the system was calibrated with and validated by use of a 3-L calibration syringe (Model 5530: Hans Rudolph, Kansas City, MO). A wide range of volumes and flow rates were delivered through the system using the super syringe to check accuracy and reliability over the typical respiratory range.

A large animal piston ventilator (Harvard Apparatus, Holliston, Massachusetts) was used to test the system for cyclical repeatability. The large animal piston ventilator is a fixed volume delivery system, which delivers the same stroke volume every time. This consistency makes it more suitable for testing purposes rather than more modern pressure-based ventilators that have a wide tolerance in delivered volume per breath. The inlet and outlets of the ventilator were connected to the system to simulate inhalation and exhalation in a complete circuit mimicking typical tidal breathing.

Following system validation tests, the volume controller was tested as part of an ongoing MDCT repeatability study using a 37-subject subset (16 Males / 21 Females, 21 Normal Non-smokers, 16 Normal Smokers; Age (years): min=20, max=64, median=27; BMI: min=18.5, max=32.0, median=23.4). The Institutional Review Board approved this study, and written informed consent was obtained from all subjects before they entered the study. Study inclusion criteria were “never smokers” (with a total smoking history of less than 1 pack-year, NS) and smokers currently smoking one pack per day. Exclusion criteria were known heart disease, kidney disease, diabetes, presence of metal in the lung field, pregnancy, an X-ray/CT scan in the past 12 months, and a body mass index over 32. NS with clinically important pathology detected on MDCT were excluded, as were smokers with significant lung disease other than emphysema. The baseline dyspnea index was determined (29). Prebronchodilator spirometry including DLCO measurements were performed via a V6200 Body Box (Sensor Medics) or an OWL body plethysmograph (Ferraris Respiratory), verified for equivalency. Spirometry quality followed the American Thoracic Society and European Respiratory Society guidelines (30).

Subjects received three volume-controlled spiral lung scans acquired during breath-holds at either total lung capacity (TLC) or functional residual capacity (FRC: designated as 20% vital capacity) measured by the volume controller. All subjects received at least one TLC and FRC scan after which they were assisted off the scanner table and permitted to walk around the room before being repositioned on the scanner for the third scan randomized to either TLC or FRC. Volumetric MDCT scan times were less than 10 seconds with a z-coverage of 22–30 cm, adjusted to capture the full apical-basal extent of the lung. Voxels were near isotropic at 0.61 mm × 0.61 mm × 0.5 mm. The following imaging protocol was used with our 64-slice MDCT scanner: 100 mAs, 120 kV, 1 mm pitch, 512 × 512 matrix, and B35f reconstruction kernel. Lung segmentation was performed on the scans using the software program PW2 (VIDA Diagnostics, Iowa City, Iowa) to assess the total CT-measured air volume within the lungs in each of the three scans. CT-measured air volumes from the repeated scans were compared using linear regression and Bland-Altman plots. The CT-measured air volume difference (CTVD) between repeated scans (i.e. CT-measured air volume from TLC scan 2 minus TLC scan 1) was calculated and compared to the analogous air volume difference recorded from the volume controller (VCVD) using linear regression, Bland-Altman plots, and Pearson correlation (statistical significance assessed for $P < 0.05$). Additional dependent variables of height, weight, age, sex, inflation level (FRC or TLC), smoker status, CT technician and volume controller operator were included in the linear regression model. Statistical analysis was performed using SPSS (IBM SPSS Version 19: IBM, Armonk, New York).

Dynamic Lung Volume Control

To achieve dynamic lung volume control that permits intermittent breath-holds for image acquisition, an enhanced version of the turbine-based breath-hold system was developed and tested. As seen in the results, this solution was inadequate and necessitated the development of an additional system better suited to dynamic lung volume control that incorporated a dual rolling-seal piston design.

Turbine-based Dynamic System Design—The turbine-based system for lung volume control during static breath-hold was enhanced to facilitate lung volume control during dynamic imaging (Figure 4). A pneumatic 3-way valve (8500 series: Hans Rudolph, Shawnee, KS) with a prefilled bag of 30% Xe / 70% O₂ attached to one side was positioned at the end of the circuit to control the inspired gas composition. Additionally two giant one-way valves (5800 series: Hans Rudolph, Shawnee, KS) were added to control the direction of gas movement and prevent rebreathing from the circuit aiming to achieve a consistent inspired gas composition between breaths. Finally, an LCD screen with readout of respiratory rate and lung volume was positioned above the subject's head to allow them to monitor and adjust their depth of breathing. The principle of the system was that subjects could monitor their lung volume on a breath-by-breath basis and adjust as needed.

Dual Piston-Based Dynamic System Design—To lessen the responsibility of the subjects to synchronize respiration and depth of breathing to a feedback system, a second system was designed specifically to control the volume of air inspired and expired on a breath-by-breath basis (Figure 5). The system employs a dual-piston reservoir design that separates the control of inspiration from expiration. The pistons, fabricated from Plexiglas, each employ a dual rolling seal design to ensure a smooth low-resistance chamber. Each piston has a linear variable differential transformer (LD620 Series: Omega, Stamford, CT) attached to the piston to measure piston displacement. A system of solenoid valves controls input gas and vacuum sources. Pneumatic shutter and three-way valves (4200 series & 8500 series: Hans Rudolph, Shawnee, KS) coupled with giant one-way valves (5800 series: Hans Rudolph, Shawnee, KS) coordinate the breathing cycle through a LabVIEW based computer control system. Initial tidal volume settings are estimated based on patient size and prior pulmonary function tests and can be easily adjusted by the system operator during a brief training session with each subject. Subjects begin with a series of deep inspirations used for lung recruitment followed by coaching to their FRC lung volume at which point they are asked to place the mouthpiece in their mouth so the system can assert control over their breathing cycle. As the subject begins to inhale, the expiratory reservoir is evacuated by the vacuum source. Once the pre-set tidal volume is fully inhaled the system closes the mouth shutter and switches the 3-way valve to permit exhalation while beginning to refill the inhalation reservoir from the appropriate gas source. Typically, the initial three breaths consist of room air followed by 17 breaths of a xenon-oxygen mixture (30% Xe, 70% O₂). Once exhalation is complete the three-way valve switches back to the inspiratory reservoir closing the respiratory circuit. At this point the scanner is triggered and images are acquired. Once complete the mouth shutter opens to allow the inspiration process to begin again.

Dynamic Systems Calibration and Testing—Both dynamic systems were validated with the 3-L calibration syringe (Model 5530: Hans Rudolf, Kansas City, MO) using a variety of tidal volumes and respiratory rates.

Following calibration and testing, the dynamic lung volume controllers were utilized to facilitate the wash-in xenon-CT method to obtain regional ventilation measurements as part of an ongoing effort to establish a normative lung atlas. This effort included a 6-subject subset (1 Male / 5 Females, 4 Normal Non-Smokers, 2 Normal Smokers; Age (years): min=21, max=44, median=24; BMI: min=18.8, max=31.4, median=26.7) using the turbine-based dynamic system, and a 41-subject subset (20 Males / 21 Females, 34 Normal Non-smokers, 7 Normal Smokers; Age (years): min=20, max=73, median=30; BMI: min=19.6, max=32.7, median=25.3) using the dual piston-based system. The Institutional Review Board approved this study, and written informed consent was obtained from all subjects before they entered the study. Study inclusion criteria were the same as the described earlier for the MDCT repeatability study.

Subjects received a dynamic volume-controlled axial lung scan consisting of 20 time points scanned during brief end-expiratory breath-holds at FRC. Scan times varied between 1 to 3 minutes, dependent on subject specific respiratory rates, with a z-coverage of 3 cm positioned between the carina and the diaphragm. Voxel sizes were around $0.61 \text{ mm} \times 0.61 \text{ mm} \times 1.2 \text{ mm}$ depending on field of view. The following imaging protocol was used with our 64-slice MDCT scanner: 150 mAs, 80 kV, 0.375 sec rotation time, 512×512 matrix, and B35f reconstruction kernel. The density change over time in each lung parenchymal voxel in the series was determined and fit to an exponential model, the time constant of which is equal to the inverse of the voxel-specific ventilation, as previously described (31). Lung segmentation and regional ventilation analysis was performed on the scans using Pulmonary Analysis Software Suite (PASS) (32).

The Institutional Review Board approved all studies reported here.

Results

Turbine-Based Breath-hold System

The system accurately controlled lung volume for 32 out of 37 subjects that complied with coaching procedures. 5 subjects were excluded from evaluation because of protocol deviations including an inadequate seal around the mouthpiece, or not following coaching procedures. The difference of VCVD subtracted from CTVD normalized to represent a percentage of CT measured air volume was $0.7 \pm 2.85\%$. The difference between VCVD from CTVD likely represents non-compliance of the subject in one form or another, including loss of air around the mouthpiece. This measure of “non-compliance” was not explained by height, weight, age, gender, smoking status, lung capacity, CT technician or volume controller operator as demonstrated in Table 1. Figure 6 demonstrates the relationship of CT measured air volume between repeated scans. For TLC and FRC scans combined (*top-left panel*) there was a linear relationship with a slope=0.9953, R-squared=0.99797; for TLC alone (*middle-left panel*), a slope=1.0252, R-squared=0.99391; for FRC alone (*bottom-left panel*), a slope=0.9664, R-squared=0.97156. The middle and right columns of Figure 6 show corresponding *Bland-Altman* plots and *difference value histogram* plots for each group. From the Bland-Altman plots in Figure 6 the mean and confidence interval of the differences (scan1-scan2) for TLC and FRC combined was -9 ml ($-169, 151$); for TLC alone 6 ml ($-164, 177$); for FRC alone, -23 ml ($-172, 126$).

As shown in Figure 7, the relationship between CTVD and VCVD was examined; there was a linear relationship with a slope=0.7037, R-squared=0.4589. Similar to Figure 6, the middle and right columns of Figure 7 show Bland-Altman and difference value histogram plots the CTVD versus VCVD comparison. The Pearson correlation coefficient showed moderate positive relationship between CTVD and VCVD ($r = 0.677$, $P < 0.0001$) between differences in repeat scan volumes using the volume controller versus MDCT. Because of the non-linear nature of the lung pressure-volume curve whereby the lung becomes stiffer at volumes near TLC, a difference in lung volume at TLC results in a smaller density change than a similar volume change near FRC. We observed that the mean lung density at TLC of the repeat scan remained within 1.5% of scan one and at FRC within 2.25% of scan one with a mean difference for both TLC and FRC being -0.27% (scan1-scan2).

Turbine-Based Dynamic System

As demonstrated in the top panel of Figure 8, failures of the turbine system were more common. When end-expiratory lung volumes fluctuated they often trended in a particular direction. As seen in this example, a downward shift in lung density is noticeable in the time vs. density curve from the turbine-based system. Once the subject began inhaling xenon gas,

they became distracted and no longer maintained an adequate seal around the mouthpiece resulting in a greater volume of inspired versus expired gas causing the end-expiratory lung volume to increase resulting in a decrease in lung density over time; contrary to the expected increase in density over time expected with the buildup of xenon gas.

While testing of the enhancements to the turbine-based system to enable dynamic lung volume control indicated that a trained operator could maintain a consistent lung volume over time, the majority of recruited subjects had moderate difficulty. None of the resulting images from the six subjects utilizing the turbine-based system for dynamic lung volume control were suitable for wash-in xenon-CT analysis.

Dual-Piston-Based Dynamic System

The dual-piston system has been better tolerated and has successfully facilitated dynamic wash-in xenon-CT studies in 31 out of 41 human subjects. Failures were due, most commonly, to subjects not following verbal instructions or proper procedures, predominantly resulting in an inadequate seal around the mouthpiece preventing the system from accurately controlling lung volume.

When the system worked, a repeatable end-expiratory lung volume was achieved and can be verified by examining the improved time versus density curves from these subjects. An example set of curves from a subject using the dual-piston system are displayed in the lower row / middle panel of Figure 8. With the improved regional curve fits, one can also observe a greatly improved color-map reflecting regional sensitivity to local lung function differences (*right panel*). Gravitational gradients in lung density are evident by the incremental shift of baseline density demonstrated by the early time points of the regional time-density curves displayed in the middle column of Figure 8 whereby the non-dependent lung region is more expanded than the dependent region at FRC. Additionally, the wash-in rate seen the lower middle panel is considerably slower (ventilation is reduced) in the non-dependent lung region, consistent with known physiology (33). The color-map in the lower-right panel of Figure 8 also reflects the vertically oriented differences in ventilation.

Discussion

Our static volume control system presented here utilizes a turbine-based flow meter that was determined to be the best balance between the strengths and weaknesses of previously described methods. The turbine is based on the principle of impeller rotation, and is therefore only affected by the volume of gas that moves across it while unaffected by temperature, humidity, or gas composition. While suitable for static breath-hold volume control, the system was ultimately not suitable for dynamic imaging. We thus presented a second system suitable for dynamic imaging consisting of a dual set of custom rolling seal pistons. The primary purpose of the lung volume controllers, maintaining a consistent lung volume during imaging, was successfully demonstrated using both the turbine-based breath-hold system and the dual piston-based dynamic system.

The newly designed turbine-based system performed well under mechanical testing and during the in-vivo breath-hold imaging (Figure 6). As shown in Table 1, study failure (with the turbine-based static breath-hold system) was not related to a particular subject characteristic or a particular technologist, but rather was influenced by individual subject compliance with instructions. With increased technologist familiarity with the system and with instructing the subjects, success of volume control improved.

To increase subject comfort, and thus compliance, the systems were designed to incorporate a mouthpiece for subject interaction. Subjects must themselves ensure a complete seal

around the mouthpiece by biting down on the bite guards and firmly closing their lips around the mouthpiece. The system can only measure the volume of air that actually moves through the circuit. Thus, if subjects do not completely seal the circuit, the system will not accurately control lung volume. Detecting this type of leak is difficult; currently there is no way for a technician to easily identify the problem other than noticing a consistent increase or decrease in the subject's overall volume during steady-state tidal breathing. This could potentially be resolved through the use of a facemask in the future, which provides an improved seal for the circuit. However, facemasks give an increased sense of confinement and can fail to seal if subjects have facial hair. It is clearly a given that compliance in the presence of significant disease will be less. It is our belief that such a system of volume control is more appropriate for subject populations in which quantitation of early disease and disease progression is sought.

The VMM-400 manufacturer specifications indicate optimal linearity of measurements in the 0.2 – 2.0 L/s flow rate range ($\pm 1.5\%$ of reading) and an accuracy of $\pm 1.5\%$. Above and below this range the system becomes increasingly unreliable. Therefore, specific care is required to ensure patients breathe in the appropriate flow range. This will sometimes require more than one attempt at achieving a desired volume as to ensure accuracy. The VMM-400 was designed primarily for respiratory cyclic flow, but can also be used to measure uni-directional flow. The turbine was designed to minimize friction on the impeller to allow for the measurement very low flow rates, however this creates an artifact during uni-directional flow when the rate goes to zero; the impeller continues to spin for short time causing a volume overshoot. This overshoot is flow rate dependent and is more significant at higher flow rates. Calibration and coaching can help minimize this issue by re-zeroing before each scan and limiting starts and stops and maintaining as smooth a respiratory cycle as possible.

We have observed that a flow rate indicator / warning light, letting the subject and technician know when inspiration or expiration is occurring too slowly or quickly (out of bounds for the turbine's linear range) would be useful. Additionally, a system to detect leaks around the subject's mouthpiece would likely reduce failure rates. It has been demonstrated in earlier studies that TLC is a more reproducible lung volume compared to FRC (22,34–37). Our studies show that, with the use of the turbine volume controller (Figure 6), the difference between TLC and FRC repeatability is negligible, yielding r^2 values of 0.99391 vs. 0.97156 respectively. This translated to a mean density (HU) difference for both TLC and FRC being -0.27% (scan1-scan2). It has been common to convert HU to g/L in evaluating emphysema progression. Using the equation $pixel\ density = 994\ (g/L) \times (1 + (HU/1000))$, the mean difference and standard error of the mean of lung density repeatability at total lung capacity using the volume controller was $-0.63 \pm 1.06\ g/L$. Dirksen et al. ((38)) reported that progression of lung density loss in untreated α_1 -antitrypsin deficient patients is on the order of $2.6 \pm 0.41\ g/L/year$ compared to $1.9 \pm 0.41\ g/L/year$ in a treatment arm. Despite using a pneumotachometer during imaging, lung volume differences were large enough as to require use of correction factors. The repeatability of the method reported here suggests that detection of yearly lung density changes is feasible without the need for corrective measures associated with inconsistent lung volumes.

The dual-piston dynamic lung volume control system successfully controlled lung volume in 31 out of 41 subjects, a considerable improvement over the success rate experienced with the turbine-based dynamic system or cases in which lung volume control was not used. The failure to control lung volume from breath-to-breath was not due to any technical or mechanical problems inherent in the system design but rather was a function of subject non-compliance in following instructions or proper procedures. Again, maintaining an adequate seal around a mouthpiece requires subjects to sustain proper focus on their breathing, a task

that can be difficult for extended periods. The slight anesthetic effects of xenon make focusing and following instructions more difficult. This often resulted in proper lung volume control during the baseline breaths and initial xenon wash-in phase but loss of compliance as the levels of systemic absorption of xenon increased. Empirically, we have found that the number of scans can be significantly reduced by eliminating some of the later time points that were often excluded because of subject non-compliance. The wash-in xenon-CT scanning protocol for the 41 subjects in this study was comprised of 3 baseline and 17 xenon wash-in breaths. By reducing the number of baseline scans from 3 to 2 and reducing the wash-in phase from 17 scans to 12, we have been able to reduce the radiation dose by 30%.

We recognized that the wash-in xenon-CT method presented here is likely too complicated for routine clinical use. However, when performed properly it provides considerable information about regional lung function, including influences of heterogeneous resistance of various forms that may not be obvious from a single inspiratory maneuver. The strength of the method presented lies in the fact that it provides a dynamic protocol against which newer, more clinically feasible, single breath dual-energy xenon-CT, can be compared.

This study demonstrated that if care is taken, one is able to coach patients to a standardized lung volume. Because lung density and airway metrics are lung volume dependent, the standardization of lung volumes during imaging is required for both cross sectional as well as longitudinally designed studies.

Acknowledgments

Funding:

This study was supported, in part, by NIH RO1-HL-064368. RG was supported through a fellowship from the Doris Duke Charitable Foundation.

We would like to thank Siemens Medical for their continued support, in particular our onsite research contact Andrew Primak. Also we would like to thank Joanie Wilson, Heather Baumhauer, and Jered P. Sieren for their efforts in subject recruitment, pulmonary function testing and training of subjects prior to and during imaging sessions.

References

1. Lynch DA, Newell JD. Quantitative imaging of COPD. *J Thorac Imaging*. 2009 Aug; 24(3):189–194. [PubMed: 19704322]
2. Aberle DR, Berg CD, Black WC, Church TR, Fagerstrom RM, et al. National Lung Screening Trial Research Team. The National Lung Screening Trial: overview and study design. *Radiology*. 2011 Jan; 258(1):243–253. [PubMed: 21045183]
3. Kim WJ, Hoffman EA, Reilly J, Hersh C, Demeo D, Washko G, et al. Association of COPD candidate genes with computed tomography emphysema and airway phenotypes in severe COPD. *Eur Respir J*. 2011 Jan; 37(1):39–43. [PubMed: 20525719]
4. Brown M, Abtin F, Kim HJ, McNitt-Gray M, Goldin JG. Imaging biomarkers for patient selection and treatment planning in emphysema. *Imaging in Medicine*. 2010 Oct; 2(5):565–573.
5. Buckler AJ, Mozley PD, Schwartz L, Petrick N, McNitt-Gray M, Fenimore C, et al. Volumetric CT in lung cancer: an example for the qualification of imaging as a biomarker. *Academic Radiology*. 2010 Jan.;107–115. [PubMed: 19969254]
6. Bafadhel M, Umar I, Gupta S, Raj JV, Vara DD, Entwisle JJ, et al. The Role of CT Scanning in Multidimensional Phenotyping of COPD. *Chest*. 2011 Sep 5; 140(3):634–642. [PubMed: 21454400]
7. Goldin JG. Imaging the lungs in patients with pulmonary emphysema. *J Thorac Imaging*. 2009 Aug; 24(3):163–170. [PubMed: 19704319]

8. Newell JD. Quantitative computed tomography of lung parenchyma in chronic obstructive pulmonary disease: an overview. *Proceedings of the American Thoracic Society*. 2008 Dec 15; 5(9): 915–918. [PubMed: 19056716]
9. Madani A, Van Muylem A, Gevenois PA. Pulmonary Emphysema: Effect of Lung Volume on Objective Quantification at Thin-Section CT. *Radiology*. 2010 Sep 17; 257(1):260–268. [PubMed: 20663967]
10. Shaker S, Dirksen A, Laursen LC, Skovgaard L, Holstein Rathlou NH. Volume adjustment of lung density by computed tomography scans in patients with emphysema. *Acta Radiologica Royal Society of Medicine*. 2004; 45(4):417–423.
11. Stoel BC, Putter H, Bakker ME, Dirksen A, Stockley RA, Piitulainen E, et al. Volume correction in computed tomography densitometry for follow-up studies on pulmonary emphysema. *Proceedings of the American Thoracic Society*. 2008 Dec 15; 5(9):919–924. [PubMed: 19056717]
12. Hoffman EA, Chon D. Computed tomography studies of lung ventilation and perfusion. *Proceedings of the American Thoracic Society*. 2005; 2(6):492–8. 506. [PubMed: 16352755]
13. Chon D, Simon BA, Beck KC, Shikata H, Saba OI, Won C, et al. Differences in regional wash-in and wash-out time constants for xenon-CT ventilation studies. *Respiratory Physiology & Neurobiology*. 2005 Aug 25; 148(1–2):65–83. [PubMed: 16061426]
14. Fuld M, Easley RB, Saba OI, Chon D, Reinhardt JM, Hoffman EA, et al. CT-measured regional specific volume change reflects regional ventilation in supine sheep. *J Appl Physiol*. 2008 Apr; 104(4):1177–1184. [PubMed: 18258804]
15. Tajik JK, Chon D, Won C, Tran BQ, Hoffman EA. Subsecond multisection CT of regional pulmonary ventilation. *Academic Radiology*. 2002 Feb; 9(2):130–146. [PubMed: 11918366]
16. Lachmann B, Armbruster S, Schairer W, Landstra M, Trouwborst A, Van Daal GJ, et al. Safety and efficacy of xenon in routine use as an inhalational anaesthetic. *Lancet*. 1990 Jun 16; 335(8703):1413–1415. [PubMed: 1972207]
17. Jordan BD, Wright EL. Xenon as an anesthetic agent. *AANA J*. 2010 Oct; 78(5):387–392. [PubMed: 21067086]
18. Chon D, Beck KC, Simon BA, Shikata H, Saba OI, Hoffman EA. Effect of low-xenon and krypton supplementation on signal/noise of regional CT-based ventilation measurements. *J Appl Physiol*. 2007 Apr 1; 102(4):1535–1544. [PubMed: 17122371]
19. Honda N, Osada H, Watanabe W, Nakayama M, Nishimura K, Krauss B, et al. Imaging of Ventilation with Dual-Energy CT during Breath Hold after Single Vital-Capacity Inspiration of Stable Xenon. *Radiology*. 2011 Oct 24.
20. Fuld M, Hudson M, Halaweish A. Quantification Of Regional Ventilation Via Dual Energy Xenon MDCT. *Am J Respir Crit Care Med*. 2010; 181:A5525.
21. Stolk J, Dirksen A, Van Der Lugt A, Hutsebaut J, Mathieu J, De REE J, et al. Repeatability of Lung Density Measurements with Low-Dose Computed Tomography in Subjects with [alpha]-1-Antitrypsin Deficiency-Associated Emphysema. *Investigative Radiology*. 2001; 36(11):648. [PubMed: 11606842]
22. Kalender WA, Rienmüller R, Seissler W, Behr J, Welke M, Fichte H. Measurement of pulmonary parenchymal attenuation: use of spirometric gating with quantitative CT. *Radiology*. 1990 Apr; 175(1):265–268. [PubMed: 2315492]
23. Orlandi I, Moroni C, Camiciottoli G, Bartolucci M, Pistolesi M, Villari N, et al. Chronic obstructive pulmonary disease: thin-section CT measurement of airway wall thickness and lung attenuation. *Radiology*. 2005 Feb; 234(2):604–610. [PubMed: 15671010]
24. Dirksen A, Piitulainen E, Parr DG, Deng C, Wencker M, Shaker SB, et al. Exploring the role of CT densitometry: a randomised study of augmentation therapy in alpha1-antitrypsin deficiency. *Eur Respir J*. 2009 Jun; 33(6):1345–1353. [PubMed: 19196813]
25. Camiciottoli G, Bartolucci M, Maluccio NM, Moroni C, Mascalchi M, Giuntini C, et al. Spirometrically gated high-resolution CT findings in COPD: lung attenuation vs lung function and dyspnea severity. *Chest*. 2006 Mar; 129(3):558–564. [PubMed: 16537852]
26. Martinot-Lagarde P, Sartene R, Mathieu M, Durand G. What does inductance plethysmography really measure? *J Appl Physiol*. 1988 Apr; 64(4):1749–1756. [PubMed: 3379007]

27. Konno K, Mead J. Measurement of the separate volume changes of rib cage and abdomen during breathing. *Journal of Applied Physiology*. 1967 Mar; 22(3):407–422. [PubMed: 4225383]
28. Hager DN, Fuld M, Kaczka DW, Fessler HE, Brower RG, Simon BA. Four methods of measuring tidal volume during high-frequency oscillatory ventilation. *Crit Care Med*. 2006 Mar 1; 34(3):751–757. [PubMed: 16505661]
29. Mahler D, Weinberg D, Wells C, Feinstein A. The measurement of dyspnea. Contents, interobserver agreement, and physiologic correlates of two new clinical indexes. *Chest*. 1984 Jun 1; 85(6):751–758. [PubMed: 6723384]
30. Miller MR, Hankinson J, Brusasco V, Burgos F, Casaburi R, Coates A, et al. Standardisation of spirometry. *Eur Respir J*. 2005:319–338. [PubMed: 16055882]
31. Simon BA, Marcucci C, Fung M, Lele SR. Parameter estimation and confidence intervals for Xe-CT ventilation studies: a Monte Carlo approach. *J Appl Physiol*. 1998 Feb; 84(2):709–716. [PubMed: 9475884]
32. Guo, J.; Fuld, M.; Alford, SK.; Reinhardt, JM.; Hoffman, EA. In: Brown, M.; de Bruijne, M.; van Ginneken, B.; Kiraly, A.; Kuhnigk, J-M.; Lorenz, C.; Mori, K.; Reinhardt, JM., editors. *Pulmonary Analysis Software Suite 9.0 Integrating quantitative measures of function with structural analyses; First International Workshop on Pulmonary Image Analysis; 2008*. p. 283-292.
33. Milic-Emili J, Henderson JA, Dolovich MB, Trop D, KANEKO K. Regional distribution of inspired gas in the lung. *Journal of Applied Physiology*. 1966 May 1; 21(3):749–759. [PubMed: 5912744]
34. Lamers R, Kemerink G, Drent M, Van Engelshoven J. Reproducibility of spirometrically controlled CT lung densitometry in a clinical setting. *Eur Respir J Eur Respiratory Soc*. 1998; 11(4):942–945.
35. Lamers RJ, Thelissen GR, Kessels AG, Wouters EF, van Engelshoven JM. Chronic obstructive pulmonary disease: evaluation with spirometrically controlled CT lung densitometry. *Radiology*. 1994 Oct; 193(1):109–113. [PubMed: 8090878]
36. Robinson PJ, Kreef L. Pulmonary tissue attenuation with computed tomography: comparison of inspiration and expiration scans. *J Comput Assist Tomogr*. 1979 Dec; 3(6):740–748. [PubMed: 512106]
37. Kohz P, Stäbler A, Beinert T, Behr J, Egge T, Heuck A, et al. Reproducibility of quantitative, spirometrically controlled CT. *Radiology*. 1995 Nov; 197(2):539–542. [PubMed: 7480708]
38. Dirksen A, Dijkman JH, Madsen F, Stoel B, Hutchison DC, Ulrik CS, et al. A randomized clinical trial of alpha(1)-antitrypsin augmentation therapy. *Am J Respir Crit Care Med*. 1999 Nov; 160(5 Pt 1):1468–1472. [PubMed: 10556107]



Figure 1. Components of the turbine-based breath-hold lung volume controller: overall system (*top panel*); Interface USA, VMM-400 turbine-based flow meter (*bottom-left panel*); Hans Rudolph two-way balloon occlusion valve (*bottom-right panel*).

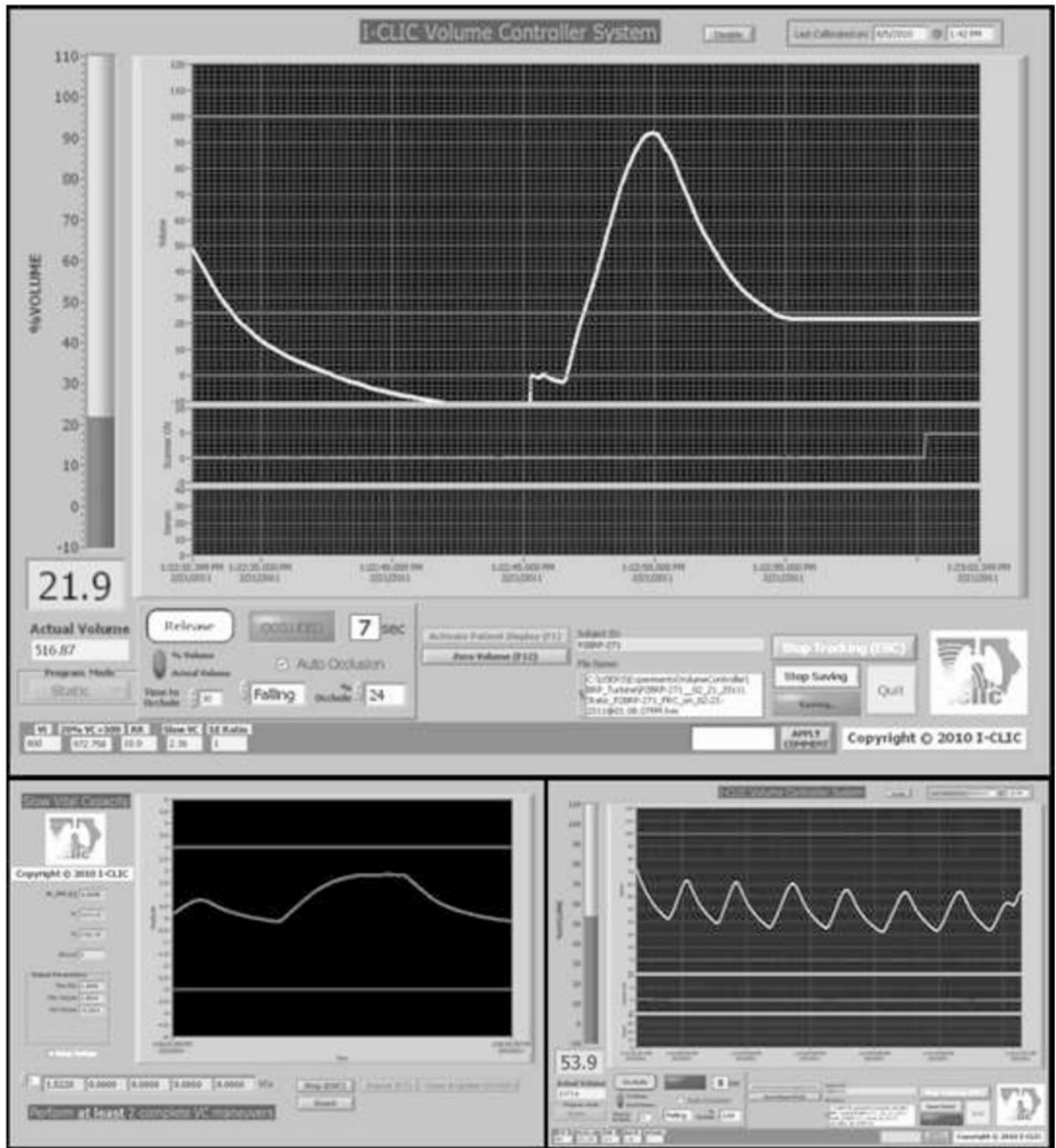


Figure 2. Screenshots of the LabVIEW control interface, during an FRC scan (*top panel*), during SVC calibration (*bottom-left panel*), and during tidal breathing (*bottom-right panel*).

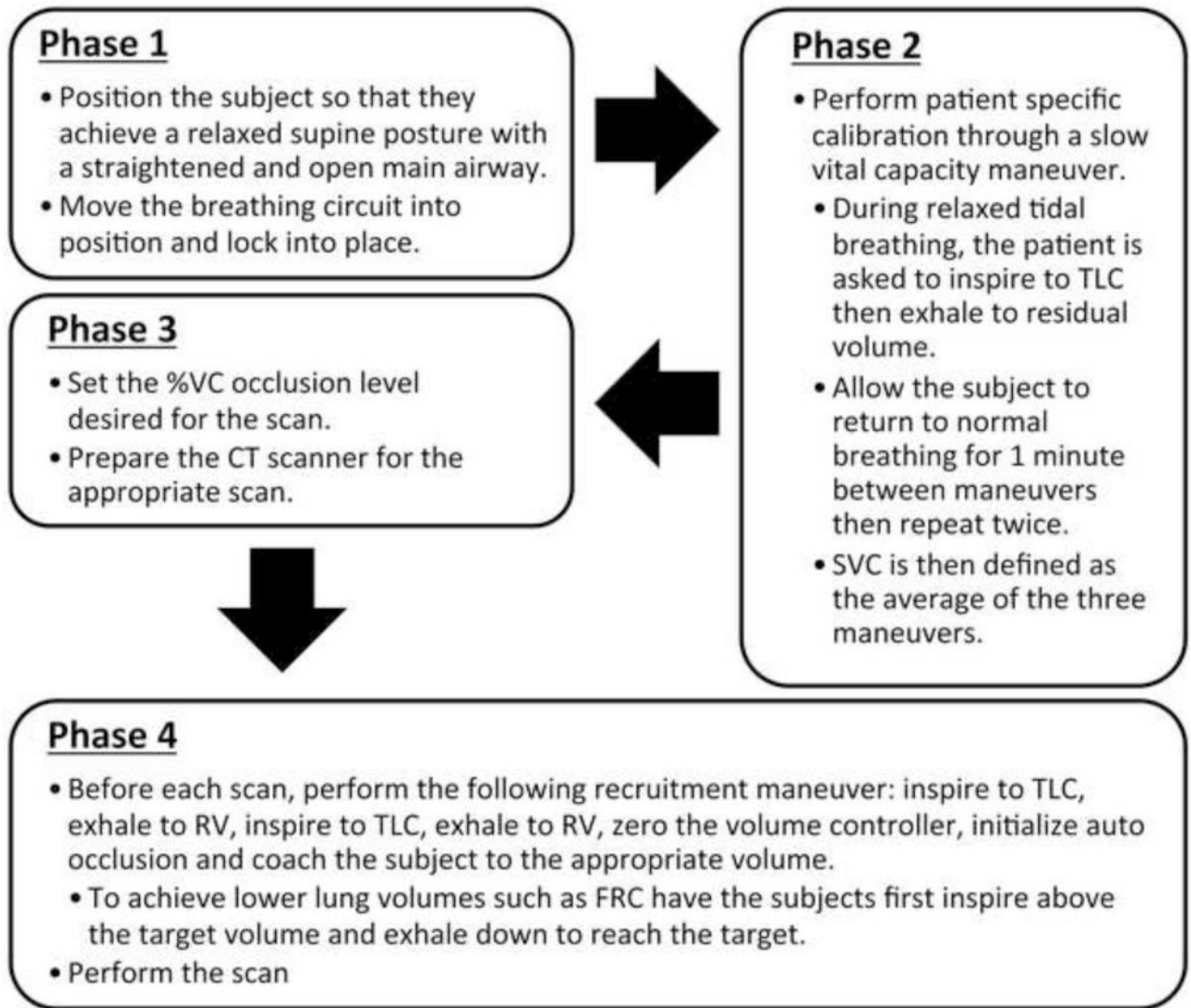


Figure 3.
Flow diagram of turbine-based breath-hold volume controller usage.

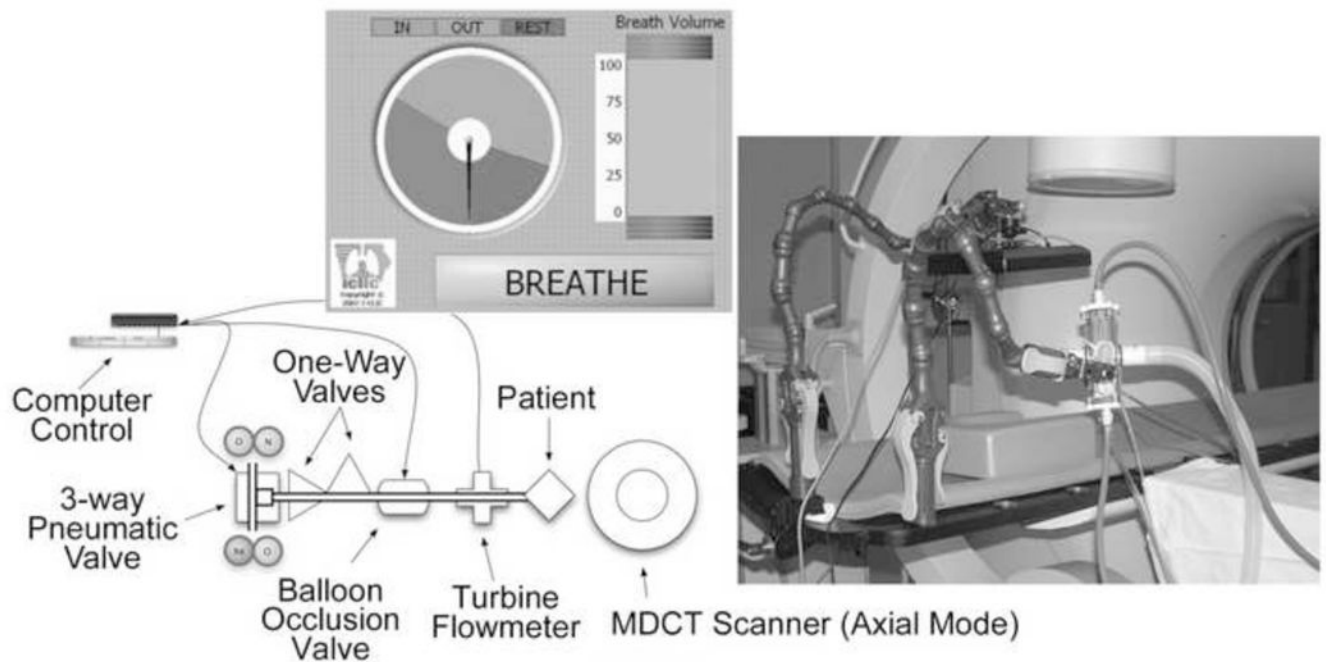


Figure 4. Adaptation of the turbine-based breath-hold volume controller for dynamic xenon-MDCT. CIVCO's "Imaging Overlay" which is made of carbon fiber with a foam core is positioned onto the scanner table which in turn allows for the attachment of CIVCO multi-articulated arms to custom fit the volume control's patient interface so that the subject can comfortably bite down on the system mouthpiece (*right panel*). A second multi-articulated arm is used to hold the display screen used to help guide the subject regarding inspiratory timing and depth of breathing (*left panel*).

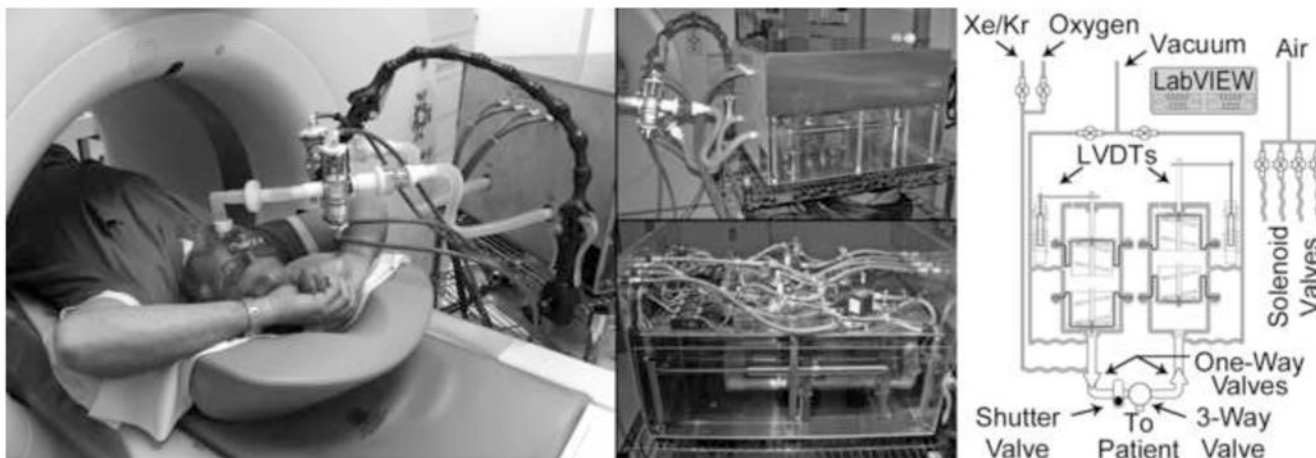


Figure 5.

Photograph and schematic diagram of the dual-piston rolling seal volume controller. During a wash-in xenon-CT study, the system is situated next to scanner table with the subject positioned inside the gantry for axial image acquisition (*left panel*). The lower portion of the system casing (*middle-top panel*) is composed of Plexiglas to allow visualization of piston motion by the system operator. Through the Plexiglas casing, the separate Plexiglas rolling seal pistons can be seen with their LVDTs positioned along the side. The upper casing has been removed (*middle-bottom panel*) to reveal the system's internal components including electronics and solenoid valves. A simplified schematic diagram illustrates individual component connectivity (*right panel*).

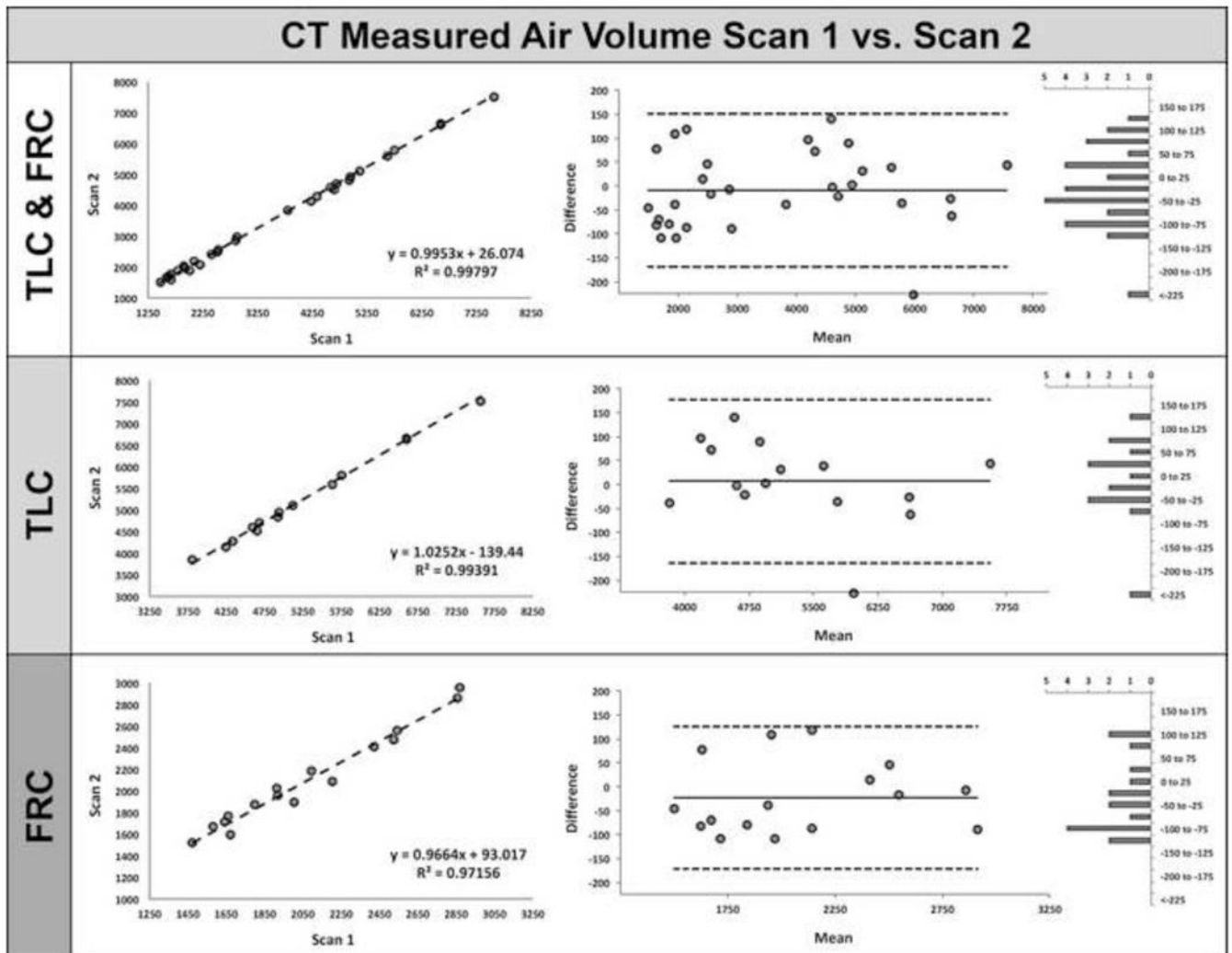


Figure 6. MDCT measured air volume correlates well between repeated scans utilizing the turbine-based breath-hold lung volume controller. Plots of CT-measured air volume comparing scan 1 vs. scan 2 for TLC & FRC combined (*left-top panel*), TLC (*left-middle panel*), and FRC (*left-bottom panel*). The middle and right columns show corresponding Bland-Altman and difference value histogram plots for each group.

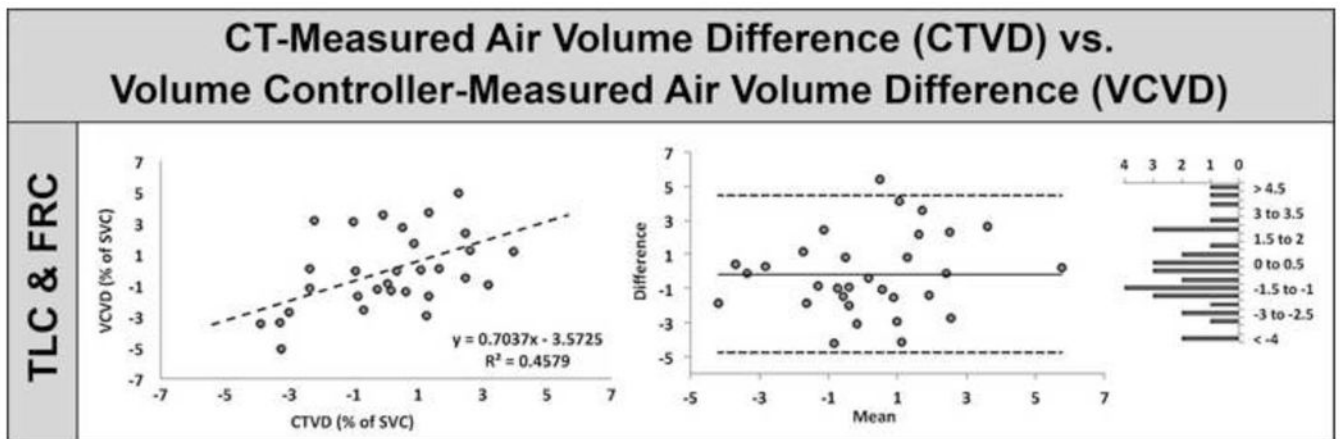


Figure 7.

The CT-measured air volume difference (CTVD) between repeated scans correlates well with the analogous turbine-based breath-hold volume controller-measured air volume difference (VCVD). Plots of CTVD vs. VCVD for TLC & FRC combined (*left panel*), Bland-Altman (*middle panel*), and difference value histogram (*right panel*).

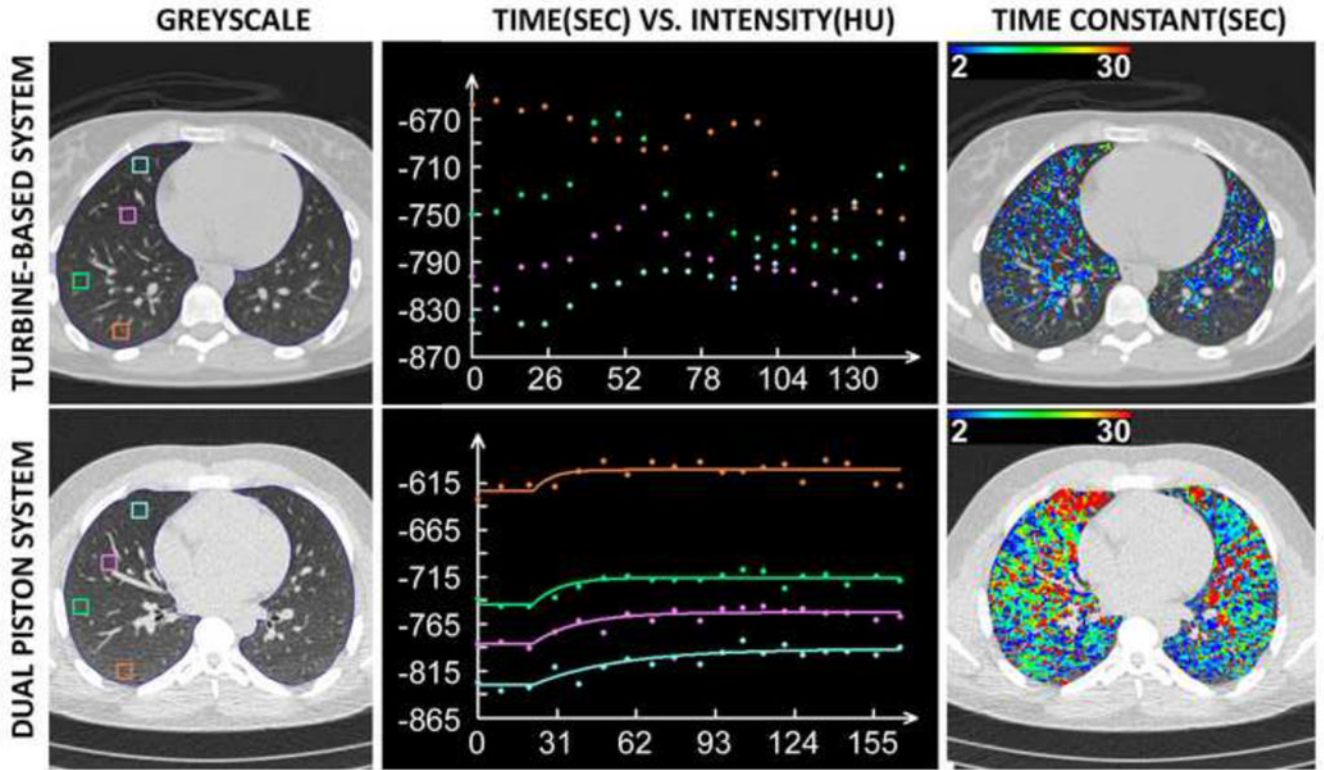


Figure 8. Wash-in xenon-CT results: The turbine-based dynamic system fails to maintain a consistent end-expiratory lung volume yielding noisy time vs. density curves (*top-middle panel*) and incorrect and incomplete color-map data (*top-right panel*). The dual-piston system more reliably controls end-expiratory lung volume yielding cleaner time vs. density curves (*bottom-middle panel*) and accurate and complete color-map data (*bottom-right panel*). Note the lower density and slower wash-in time constants (*blue curve, bottom-middle panel*) in the non-dependent vs. dependent (*orange curve, bottom-middle panel*) representing a greater lung expansion at FRC and reduced ventilation to this same region in the non-dependent lung region. This is in agreement with well-recognized heterogeneity of lung function. Despite the inconsistent lung volumes at FRC achieved by the turbine-based system, the same vertically oriented relationship in lung density is observed within the early time points.

Table 1

Results from a linear model indicate that none of the listed parameters statistically influence the difference between VCVD and CTVD.

Parameter	p-value
Height	0.876
Weight	0.336
Age	0.398
Lung Capacity	0.807
Smoking Status	0.925
Gender	0.590
CT Technician	0.351
VC Operator	0.771